SIN-CHN SCIENTIFIC PRESS PTE.LTD.

Molecular & Cellular Biomechanics 2024, 21, 133.
https://doi.org/10.62617/mcb.v21.133

Article

Finite element analysis of the biomechanical effects of anterior and posterior cervical fusion surgery for bilateral cervical dislocation

Dan Li[1], Ke Wang[1,*], Chao Dong[2], Bo Zhou[1], Lin Gu[3], Haoran Yang[4]

[1] Rail Transit Rolling Stock College, Hunan Railway Professional Technology College, Zhuzhou 412001, China
[2] CRRC ZhuZhou Institute Co. Ltd., Zhuzhou 412001, China
[3] Xiang YA Hospital Zhuzhou Central South University, Zhuzhou 412001, China
[4] The Second Hospital of Zhuzhou City, Zhuzhou 412001, China
*** Corresponding author:** Ke Wang, wangke1978_0125@163.com

CITATION

Li D, Wang K, Dong C, et al. Finite element analysis of the biomechanical effects of anterior and posterior cervical fusion surgery for bilateral cervical dislocation. Molecular & Cellular Biomechanics. 2024; 21: 133. https://doi.org/10.62617/mcb.v21.133

ARTICLE INFO

Received: 19 January 2024
Accepted: 17 April 2024
Available online: 8 May 2024

Abstract: Lower cervical spine injuries often manifest as lower cervical vertebral fractures and dislocations, as well as lower cervical facet joint dislocations. Especially in cases of bilateral facet joint dislocations, it is important to rapidly and effectively relieve spinal cord and nerve root compression to prevent secondary spinal cord injury, while also providing reliable and long-lasting stability to the injured segment after surgery. Combined anterior and posterior approaches have the advantages of both pure anterior or posterior approaches, but the actual situation is complex and variable, making systematic theoretical analysis crucial. This study, with bilateral facet joint dislocation of the C6 segment and cervical spinal cord injury as the research background, established a three-dimensional model of the cervical spine C3-C7 after implementing four types of anterior-posterior combined surgeries. The four surgical approaches consist of four combinations: anterior parallel or inclined screw placement combined with posterior Margel or Anderson method screw insertion. Through finite element method, a systematic comparative analysis of the theoretical effects of the four combined surgeries in treating bilateral facet joint dislocation of the cervical spine was conducted. The conclusion was that the variations in the four combined fixation methods have a certain impact on the biomechanical characteristics of the intervertebral disc nucleus. There is a clear mutual influence relationship among anterior and posterior fixation instruments. Based on the model used in this study, it is recommended to use a torque greater than 2.1 nm to tighten the locking nut of the posterior rod to ensure reliable internal fixation.

Keywords: Bilateral facet joint dislocation; finite element analysis; combined anterior-posterior fixation surgery; biomechanics

1. Introduction

Lower cervical spine injuries are the most common type of cervical spine injuries and often manifest as lower cervical vertebral fractures and dislocations, including facet dislocations. The treatment principles for facet dislocation of the lower cervical spine involve restoring the normal structure of the cervical spine, relieving spinal cord and nerve root compression, promoting neurological recovery, preventing secondary spinal cord injury, and achieving reliable and long-lasting stability in the injured segment [1–9].

Treatment options for bilateral facet joint dislocation in the lower cervical spine include closed cranial traction, external fixation, anterior-only fixation, posterior-only fixation, or combined anterior-posterior fixation surgery. However, the choice of treatment approach remains a contentious issue in the academic field [10–13].

Some scholars have evaluated the clinical outcomes of anterior approach surgery for reduction, decompression, and fixation of lower cervical vertebral fractures and dislocations. They have observed significant improvements in intervertebral disc height and cervical lordosis Cobb angle postoperatively. However, for some ASIA grade A or B patients, functional recovery is not satisfactory [14–16].

Other researchers have studied the effects and influencing factors of anterior plate fixation for cervical dislocation. The results suggest that this method can improve cervical function and promote joint reduction, but surgical time, postoperative Cobb angle, and complications are risk factors affecting the incidence of postoperative complications [17,18].

There have also been studies on different surgical approaches for the treatment of lower cervical vertebral fractures and dislocations combined with spinal cord injury. The results show that surgical treatment can significantly promote the recovery of spinal cord function. The outcomes of various surgical approaches are similar, with anterior approach surgery demonstrating advantages in terms of surgical time and blood loss compared to posterior approach or combined anterior-posterior approach. However, these studies lack a systematic analysis from a biomechanical and theoretical perspective [19–21].

Some scholars have compared the efficacy of two different surgical approaches, namely anterior decompression reduction and fixation surgery, for the treatment of cervical vertebral fractures and dislocations combined with spinal cord injury. They concluded that anterior decompression reduction and fixation surgery significantly improves vertebral function and has a high level of safety. However, due to small sample sizes, further validation is required.

Considering the possibility of failure in anterior approach surgery, some authors suggest performing posterior approach surgery directly or adding posterior approach reduction or fixation after anterior approach surgery. They believe that compared to anterior approach surgery, posterior approach surgery can directly release the facets, allowing for easier reduction, and the fixation with pedicle screws provides better biomechanical stability [22–24].

However, simple posterior surgery has its obvious disadvantages. For example, soft tissues such as spinal cord ventral protrusion of intervertebral disc cannot be removed before reduction. The selection of surgical approach also depends on many other factors. Whether there is concomitant traumatic intervertebral disc protrusion, whether closed reduction is successful, etc.

Some scholars also believe that simple anterior or posterior surgery may result in failure to achieve reduction, inability to relieve compression after reduction, and unreliable fixation. They summarize through relevant experiments and believe that the combined approach of anterior and posterior surgery is a more definitive surgical option for maintaining cervical stability after fracture or dislocation. And the combined approach is more recommended for bilateral dislocation or complete relief of spinal cord nerve root compression or further damage [25–30].

Although the combined approach surgery combines the advantages of simple anterior or posterior surgery, the actual situation of vertebral displacement and cervical spinal cord injury is often complex and variable. The biomechanical impact of internal fixation systems on the cervical spine needs to be quantitatively and visually studied.

The systematic theoretical analysis of anterior-posterior internal fixation surgery for the cervical spine is particularly critical [31–35].

Based on the research of the above scholars, this article intends to establish a C3-C7 cervical spine model, with bilateral facet joint dislocation of the C6 segment and cervical spinal cord injury as the research background. Through finite element analysis, a systematic analysis of the theoretical effect of anterior-posterior combined surgery for the treatment of bilateral facet joint dislocation of the cervical spine will be conducted, providing a theoretical basis for the clinical treatment of bilateral facet joint dislocation of the lower cervical spine.

2. Materials and methods

2.1. Establishment of three-dimensional models for anterior and posterior cervical internal fixation procedures

A specific model and parameters of a cervical anterior internal fixation kit were selected based on a medical device parameter in **Table 1**. The cervical internal fixation instrument is suitable for cervical instability and slippage.

Table 1. The parameters for anterior cervical internal fixation.

Device name	Type	Length (mm)	Parameter 1 (mm)	Parameter 2 (mm)
Anterior cervical titanium plate type I	11.111.01-053	53	Width 18	Thickness 2.1
Anterior cervical screw	11.111.02-616	16	Diameter 4	-

The posterior cervical internal fixation instrument model was also based on a specific model and parameters of a cervical anterior internal fixation kit in **Table 2**.

Table 2. The parameters for posterior cervical internal fixation.

Device name	Type	Length (mm)	Diameter (mm)
Cancellous Multi Axial Screws	50603512	12	Width 3.5
Rod	50690000	80	3.5
Set Screw	50694000	-	6

Combination scheme designs were performed using two different screw insertion methods for the anterior approach and two different screw insertion methods for the posterior approach, as shown in **Table 3**. Scheme A utilizes a parallel anterior approach with the Magerl method for the posterior approach. Scheme B utilizes a parallel anterior approach with the Anderson method for the posterior approach. Scheme C utilizes an oblique anterior approach with the Magerl method for the posterior approach. And Scheme D utilizes an oblique anterior approach with the Anderson method for the posterior approach.

The horizontal placement of anterior cervical plate scheme is one of the methods being studied in order to simulate the theoretical anterior horizontal screw placement in anterior cervical internal fixation surgery. On the other hand, the oblique anterior screw placement is used to replicate the actual clinical cervical injury or lesion conditions during the surgery process, where complete horizontal screw placement

cannot always be guaranteed due to various factors. In this study, based on multiple uncertain clinical factors, an angled screw placement scheme was devised as shown in **Figure 1**. Specifically, S1 screw is inserted with an upward inclination of 10 degrees and an outward inclination of 5 degrees. S2 screw is inserted with an upward inclination of 10 degrees. S3 screw is inserted with a downward inclination of 10 degrees and an inward inclination of 5 degrees. S4 screw is inserted with a downward inclination of 10 degrees.

Table 3. The theoretical combination schemes for the anterior and posterior approaches.

Approach method	Nailing mode	Combined operation scheme			
		A	B	C	D
Parallel	Anterior cervical approach with the ideal parallel angle.	◎	◎		
Oblique	Anterior cervical approach considering actual circumstances, as shown in **Figure 1**.			◎	◎
Magerl	Inward by 2–3 mm from center, oblique outward by 30 degrees, depth 13.8 mm–16 mm [36–38].	◎		◎	
Anderson	Inward by 1 mm from the center, oblique outward by 10 degrees, upward by 30–40 degrees, depth 16 mm–18 mm [39].		◎		◎

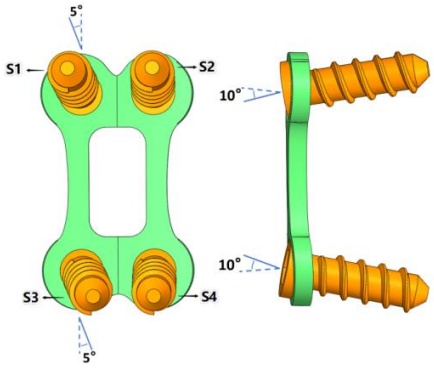

Figure 1. Angle plan for oblique placement of anterior approach nails.

According to the specific parameters provided in **Tables 1** and **2**, the solid models of each component were drawn using Solidworks 3D modeling software. The titanium plate model retains the anatomical arc-shaped design features of the original instrument, which allows for a more realistic simulation of the interaction between the postoperative internal fixation system and the anterior cervical approach. Following the surgical grouping scheme described in **Table 3**, the internal fixation components of each group were assembled. The three-dimensional model of the anteriorly tilted nail is shown in **Figure 1** after its establishment. Based on the CT scan data of a normal person, the C3-C7 cervical spine surface envelope model was extracted using Mimics software. It was then imported into Solidworks software, where the surfaces of each vertebral body and intervertebral disc were processed in detail, completing the surface detail optimization and closure processing of the cervical spine model. A three-dimensional solid model of the C3-C7 cervical spine was established through solidification operations. The established internal fixation assembly model was assembled with the cervical spine model according to the assembly relationship, nail insertion position, and angle. After all assembly relationships were fully constrained, all nail holes in the vertebral bodies were drilled using part feature editing. Using a

similar modeling method, the three-dimensional solid models of the cervical spine after surgery were sequentially established for four surgical schemes, as shown in **Figure 2**.

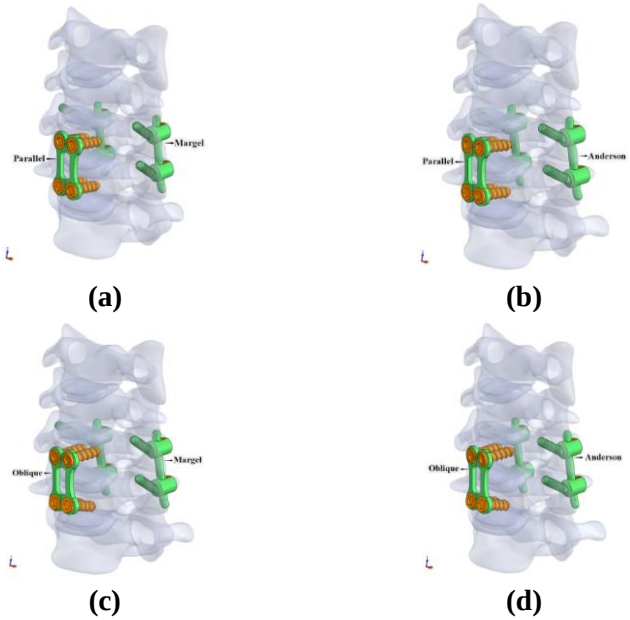

(a) **(b)** **(c)** **(d)**

Figure 2. The model after decompression and fusion surgery in the anterior approach. **(a)** scheme A; **(b)** scheme B; **(c)** scheme C; **(d)** scheme D.

2.2. Finite element model establishment of anterior and posterior internal fixation surgery

The C3-C7 three-dimensional solid model was imported into the finite element software Abaqus. Through the 2D/3D meshing function, the model was divided and meshed, generating a total of 1,273,731 meshes. The imported model retained the assembly relationship between the vertebral bodies and the internal fixation. The materials and property parameters of the cervical spine and internal fixation system are listed in **Table 4**. Among them, the cortical bone of the vertebral body is defined as a two-dimensional surface mesh, while the rest of the components are three-dimensional solid homogeneous tetrahedral meshes.

Table 4. Material properties used in the cervical spine model.

Material type	Elastic modulus (Mpa)	Poisson's ratio	Mesh type
Cortical bone	12,000	0.29	S3
Cancellous bone	100	0.29	C3D4
End plate	500	0.4	C3D4
Annulus fibrosus	3.4	0.4	C3D4
Nucleus pulposus	1	0.49	C3D4
Cartilage	10.4	0.4	C3D4
Titanium plate, screw, titanium rod (titanium alloy)	114,000	0.35	C3D4

This research model includes multiple interacting relationships, including the upper and lower endplates of the vertebral bodies with the intervertebral discs, the upper and lower articular processes of the vertebral bodies, the internal fixation screws with the vertebral bodies, and the intervertebral discs between all internal fixation instruments. These relationships are simulated by setting interaction constraints to achieve relevant connections. The establishment of the interaction model is accomplished by selecting the action areas and setting the action properties, as shown in **Figure 4a**. The interaction properties in the model include small sliding contact, binding action, and coupling action.

To more accurately replicate the biomechanical effects and mobility of the cervical spine, a finite element model incorporated an equivalent modeling of ligaments. Ligaments were defined in the finite element model of the C3-C7 segments, including the anterior longitudinal ligament, posterior longitudinal ligament, ligamentum flavum, interspinous ligament, and capsular ligament. As ligaments are fibrous tissues that can only withstand tensile loads under loading conditions, linear elements with tension-only characteristics were used. Corresponding reference points were placed on the anterior and posterior sides of the vertebral bodies, between adjacent vertebral plates, and at the ends of each spinous process. These reference points were coupled with ligament nodes in their respective regions through motion coupling. Connector elements were selected to connect the attachment regions of the ligaments represented by the reference points. Material properties were assigned based on the load-deformation curves, with material plasticity and failure regions ignored. The load-deformation curves of various ligaments in the lower cervical spine after fitting are shown in **Figure 3** [40–43]. Based on this curve data, a comprehensive ligament model of the cervical spine was established, as depicted in **Figure 4b**.

The interactions between the upper and lower endplates of vertebral bodies, upper and lower articular facets, fixation screws and vertebral bodies, as well as between the disc and vertebral bodies, were simulated by setting interaction constraints, as shown in **Figure 4a**. A comprehensive ligament model of the cervical spine was established as shown in **Figure 4b**.

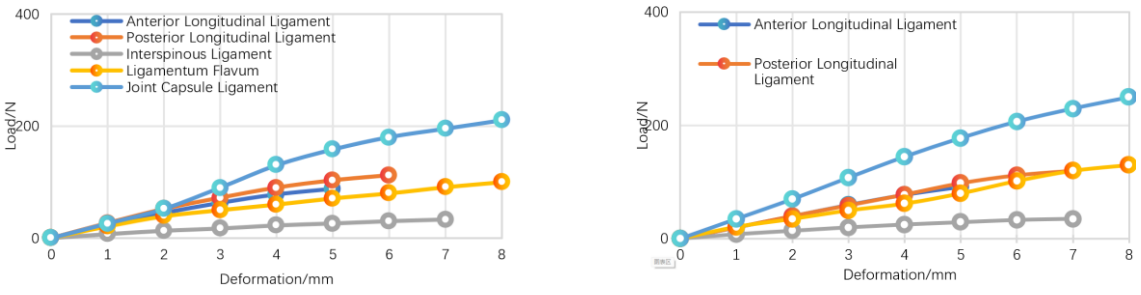

Figure 3. Curve of ligament deformation under load. **(a)** Ligament mechanical properties from C3-C5; **(b)** Ligament mechanical properties from C5-C7.

According to the motion data of the cervical spine in normal adults, a gravity load of 73.6 N was applied to the surface of the C3 vertebral body, along with a 1 nm bending moment with each motion axis as the rotation center to simulate flexion, extension, lateral bending, and rotation movements. The lower surface of the C7

vertebral body was completely constrained to simulate the relative motion between C7 and the following segments, resulting in a complete load model as shown in **Figure 4c**.

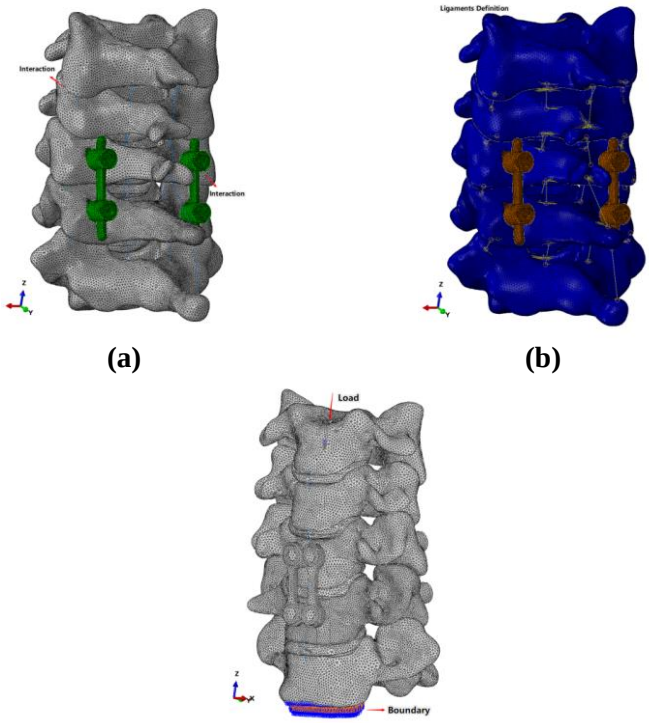

Figure 4. Finite element model after anterior decompression and fusion surgery. **(a)** interaction model; **(b)** ligament definition; **(c)** load and boundary.

3. Result

3.1. Postoperative mobility of the hybrid anterior-posterior approach in anterior cervical fixation

3.1.1. Finite element model validation

According to the previous research in this paper, the established finite element model of the C3-C7 segment of the normal human cervical spine was solved and analyzed. The range of motion (ROM) values of the intervertebral motion at the C3-C7 level were obtained based on the rotational displacement results, and compared with the experimental results [43,44]. And as shown in **Figure 5**.

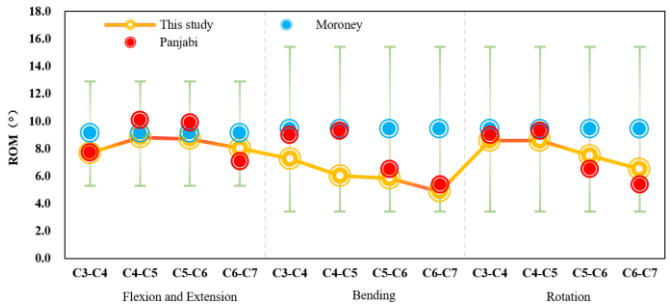

Figure 5. Comparison of intervertebral motion ROM (°) at 1 nm load on the cervical spine.

The mobility of the established cervical spine finite element model is within the normal range of deviations. The C3-C7 cervical spine finite element model has been validated effectively.

3.1.2. Postoperative mobility of the hybrid anterior-posterior approach

The finite element results of the displacement of the C5-C6 segment in the hybrid anterior-posterior approach are shown in **Figure 6**. The maximum flexion displacement of the cervical spine is approximately 26.7 mm, and the maximum axial rotation displacement is approximately 27.4 mm. It can be seen from Figure c that the intervertebral motion at the C5-C6 segment is basically zero under all cervical spine motions. In addition, there are some changes in the intervertebral motion of the other segments compared to the normal cervical spine model. Under lateral bending motion, the intervertebral motion at the C3-C4 segment is reduced due to the influence of the C5-C6 segment fusion, while the C4-C5 segment shows little change. The intervertebral motion of the C6-C7 segment changes relatively little under various conditions.

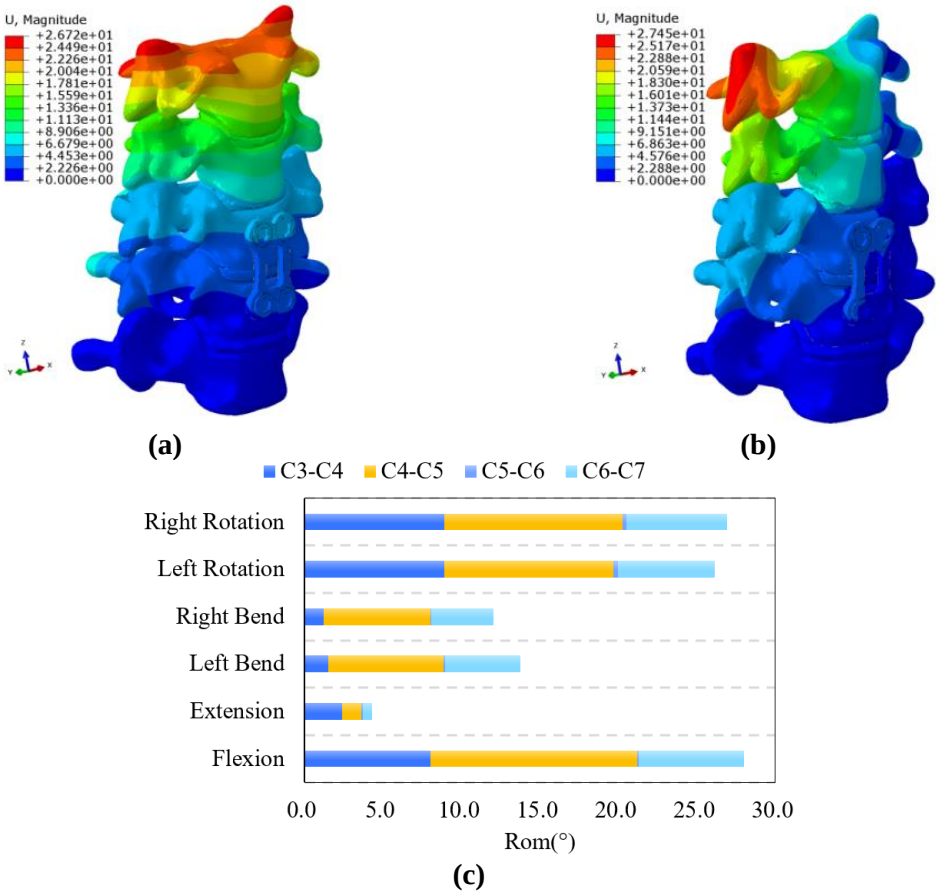

Figure 6. Nephogram of cervical displacement and results of intervertebral motion after combined anterior-posterior internal fixation. **(a)** flexion and extension; **(b)** rotation; **(c)** cervical intervertebral motion after combined operation.

3.2. Stress results of four types of combined anterior and posterior internal fixation models at levels 5-C6

The adjacent segment C4-C5 nucleus pulposus stress conditions are shown in **Figure 7** with the C5-C6 segment as the target for internal fixation. From the figure,

it can be seen that the equivalent stress distribution of the nucleus pulposus in the C4-C5 segment is basically the same for the four anterior-posterior approaches under various cervical spine motion conditions. During flexion and extension movements, the nucleus pulposus is mainly stressed on the anterior and posterior sides of the cervical spine. During lateral bending, there is obvious local stress release on the opposite side of the cervical spine movement direction. However, the stress distribution of the nucleus pulposus differs during axial rotation of the cervical spine compared to the previous movements. Regardless of left or right rotation, there is obvious local edge stress on the anterior side of the cervical spine, and the opposite side also shows significant local stress release, depending on the specific direction of the axial rotation.

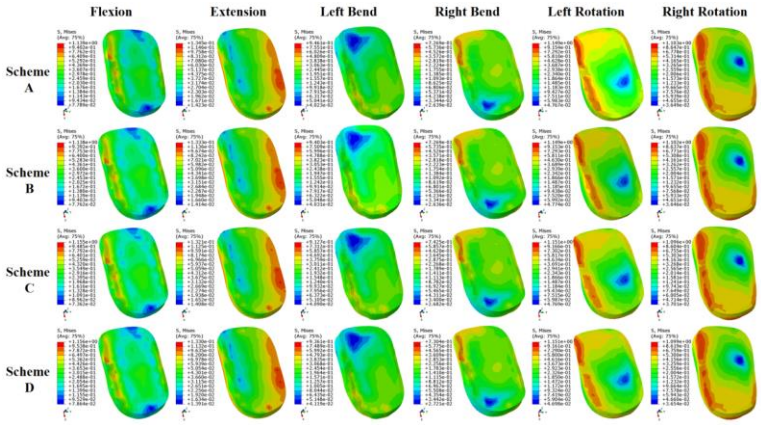

Figure 7. Equivalent stress nephogram of C4-C5 nucleus pulposus after combined internal fixation.

From the figure, it can be observed that the maximum equivalent stress of this intervertebral disc occurs during cervical flexion and axial rotation. Specifically, during flexion, both Scheme A and B have a maximum value of approximately 1.14 MPa, with an average value of 0.36 MPa. Scheme C and D have a maximum value of approximately 1.16 MPa. During left rotation, Scheme A and B have a maximum value of approximately 1.15 MPa, slightly lower than the stress values of Scheme C and D under the same conditions. During right rotation, Scheme A to D have equivalent stress values of approximately 1.10 MPa. The smaller equivalent stress of the nucleus pulposus occurs during cervical lateral bending. Specifically, during right-sided bending, Scheme A and B have a maximum equivalent stress value of approximately 0.73 MPa, slightly lower than Scheme C and D's 0.75 MPa under the same conditions. In this condition, the average stress distribution of the four methods is around 0.18 MPa. During left-sided bending, the maximum equivalent stress for all four methods is approximately 0.93 MPa, which is an average increase of 39.4% compared to the maximum stress value during right-sided bending. Scheme A has slightly higher nucleus pulposus stress than the other three methods, with a maximum value of 0.95 MPa and an average stress of approximately 0.24 MPa. The minimum equivalent stress of the C4-C5 nucleus pulposus occurs during cervical extension. The equivalent stress values for Scheme A to D are all around 0.13 MPa, a reduction of approximately 63.89% compared to the corresponding values during flexion. During

extension, the average stress values of the nucleus pulposus for all methods are approximately 0.06 MPa, a reduction of approximately 83.3% compared to the corresponding values during flexion.

The stress conditions of the adjacent segment C6-C7 nucleus pulposus are shown in **Figure 8**. From the figure, it can be seen that the equivalent stress distribution of the C6-C7 nucleus pulposus is also similar for the four anterior-posterior approaches under various cervical spine motion conditions. During cervical flexion and extension, this nucleus pulposus is mainly stressed in the central region. During lateral bending, there is noticeable stress concentration on the same side as the cervical spine movement direction. During axial rotation of the cervical spine, there is also significant local stress release on the opposite side of the nucleus pulposus, depending on the specific direction of the axial rotation.

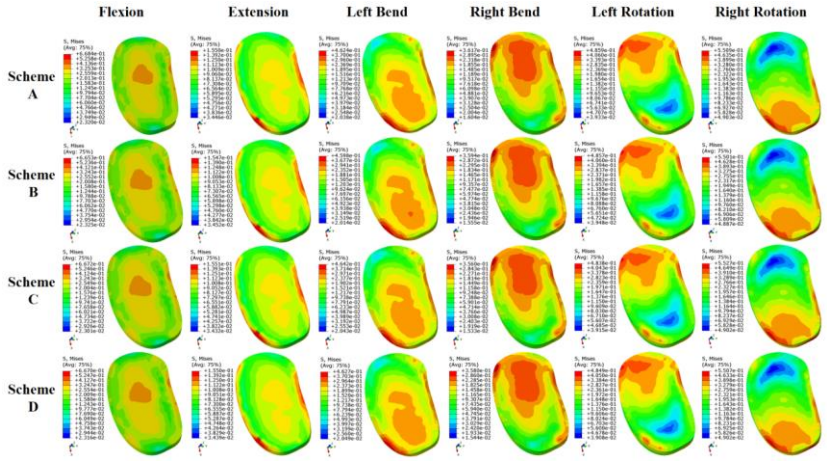

Figure 8. C6-C7 equivalent stress nephogram of nucleus pulposus after combined internal fixation.

As shown in the figure, the maximum equivalent stress value of the nucleus pulposus of the C6-C7 intervertebral disc occurs during cervical flexion, with maximum values for Scheme A-D around 0.67 MPa and an average value of 0.16 MPa. Under left rotation, the maximum stress values for all methods are around 0.48 MPa, slightly lower than those under flexion, with a reduction of about 28.4%. The average stress value is 0.17 MPa, slightly higher than that under flexion. Under right rotation, the equivalent stress of Scheme A-D is around 0.55 MPa, slightly larger than that under left rotation and about 17.9% smaller than that under flexion. The smallest equivalent stress of the nucleus pulposus in the C6-C7 intervertebral disc is consistent with the situation in C4-C5, where it occurs during cervical extension. The equivalent stress of Scheme A-D is around 0.16 MPa, about 76.1% lower than the corresponding value under flexion. The average stress is about 0.08 MPa, 50% lower than that under flexion.

It can be seen from the **Figure 9** that the stress distribution of the screw is strongly related to cervical movement, and the stress concentration area will change with the change of working conditions. During flexion, the stress concentration area of all four methods is at the threaded position of the C6 fixed screw, specifically at the 1/2 position near the screw head, showing an elliptical stress diffusion distribution. During

cervical extension, there is an obvious edge stress concentration phenomenon at the screw head position of the C5 fixed screw, which is mainly due to the axial traction and transverse shear caused by the limited position and bolt pre-tension force between the titanium plate and the upper and lower fixed screws during extension. During lateral flexion, a stress concentration phenomenon also occurs at the screw head position of the C5 fixed screw. The specific position of this working condition is directly affected by the direction of lateral flexion, with stress concentrated on the right screw head when the left side is flexed, and vice versa. During axial rotation, the stress distribution of the front screw of the four methods is directly related to the direction of rotation. Under left rotation, the stress is mainly concentrated on the left fixed screw of C6, while under right rotation, it is concentrated on the screw head of the right side.

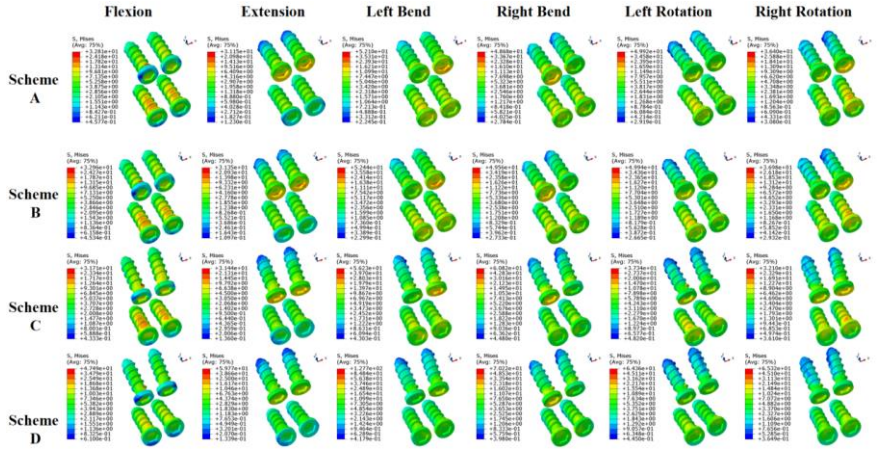

Figure 9. Equivalent stress nephograph of C5-C6 anterior internal fixation screw.

Figure 10 shows the stress curve of the front screw of the four methods after anterior-posterior combined internal fixation surgery. It can be seen from the figure that the maximum stress curve of the front screw is basically the same for all four methods. During lateral flexion, the maximum stress value of the front screw is significantly higher than that under other motion conditions. Under left lateral flexion, the maximum stress value of Scheme D reaches 127.7 MPa, about 132% higher than the corresponding values of the other three methods. Under right lateral flexion, the maximum stress of Scheme D is 70.2 MPa, about 15.4% higher than that of Scheme C. During cervical axial rotation, the maximum stress value of the front screw of the four methods is slightly smaller than that of lateral flexion, with a reduction of about 49.6% for Scheme 4 under left rotation compared to left lateral flexion. The situation is slightly lower under right rotation than under left rotation. Under flexion, the maximum stress situation is similar to that of axial rotation. The smaller stress situation of Scheme A–D occurs during cervical extension. The maximum stress values of Scheme A–C are around 31.5 MPa, about 47.3% lower than the value of Scheme D under the same working condition.

The bar chart in the figure shows the average equivalent stress of the anterior cervical screw during four different methods of cervical movements. It can be observed that the distribution trend of the stress values is consistent with the maximum stress situation. It is particularly noticeable that the average stress of Scheme D is the

same as the maximum stress, and it is higher than the other three methods in all conditions. The highest average stress occurs in the left movement, with a stress value of 10.9 MPa, while the lowest stress occurs in the extension movement, with a stress value of 4.4 MPa. Scheme C has slightly higher average stress than Scheme A and B in lateral bending movement. The average stress values of the other conditions are similar for all three methods.

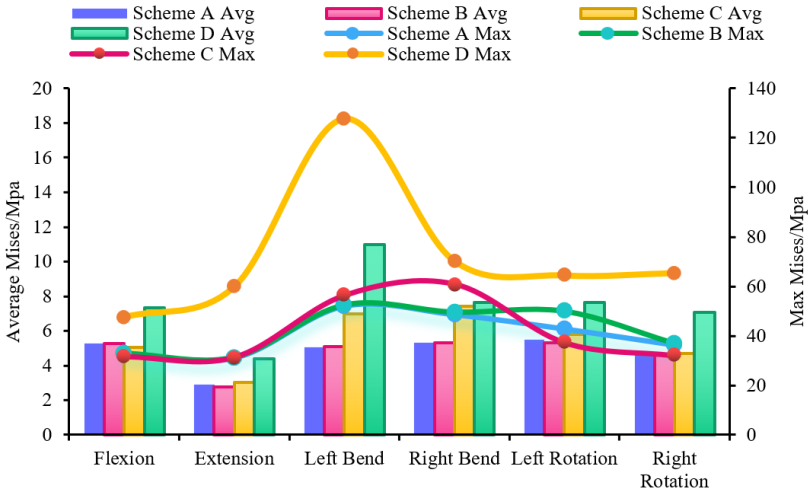

Figure 10. Stress values of the anterior screws of the four methods.

As shown in **Figure 11**, the stress distribution of the posterior screws is also related to the cervical movements. During flexion movement, the stress concentration areas of all four methods are at the connection between the two fixed screws on the right side. During cervical extension movement, stress concentration areas exist in the connection positions of all four posterior screws (Scheme A to D). During cervical lateral bending movement, the specific stress concentration positions are directly influenced by the bending direction. When bending to the left, the stress concentration occurs at the left screw connection, and when bending to the right, it occurs in the corresponding right area. The distribution pattern during axial rotation movement is similar to that during extension movement. Stress concentration areas exist in the screw-head connection positions of all four posterior screws. The stress is transmitted from the root of the thread to the outer end and gradually diminishes.

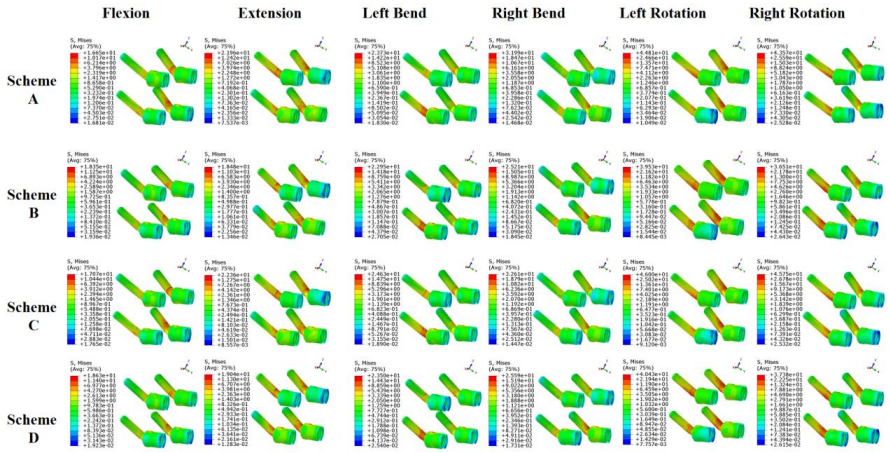

Figure 11. Equivalent stress nephograph of C5-C6 posterior internal fixation screw.

Figure 12 shows the stress curves of the posterior screws after combined anterior and posterior fixation using the four methods. It can be observed that the maximum stress curves of the posterior screws are similar for all four methods, with Scheme A and C having high degree of overlap and Scheme B and D having high degree of overlap. Unlike the anterior approach, the maximum stress condition occurs during axial rotation movement. Under left rotation, the maximum equivalent stress values for Scheme A and C are 46 MPa and 44.8 MPa, respectively, which are similar to the stress values during right rotation. Under this movement, the maximum stress values for Scheme B and D are approximately 40 MPa, which is an average reduction of 11.1% compared to Scheme A and C. For right rotation, the maximum stress values for Scheme B and D are reduced by approximately 7.5% compared to left rotation. The maximum stress values for the four methods show a decreasing trend from right to left, and from extension to flexion. Under right rotation movement, the maximum stress values for Scheme A and C are approximately 31.4 MPa, which is an increase of about 83.6% compared to their flexion movement stress of 17.1 MPa. The maximum stress values for Scheme B and D are approximately 25 MPa, which is an increase of about 33.7% compared to their flexion movement stress of 18.7 MPa.

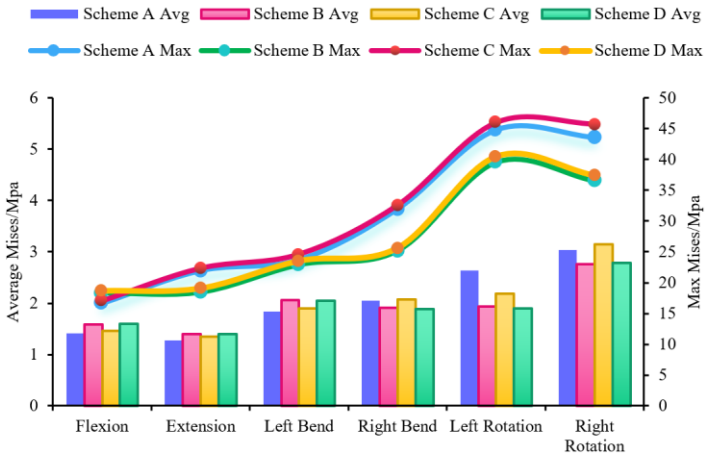

Figure 12. Stress values of the four methods of the posterior screw.

The bar chart in **Figure 12** shows that the distribution of the average stress values is consistent with the maximum stress situation and gradually decreases from right to left. The average stress values of the four methods in the same cervical movement are also consistent with their maximum stress situation. For example, during left rotation movement, the average stress values for Scheme A and C are 2.4 MPa, which is slightly larger by 26.3% compared to the corresponding values for Scheme B and D.

4. Discussion

4.1. Analysis of the biomechanical effects of four combined internal fixation methods

Figure 13 shows the stress distribution curves of adjacent intervertebral disc nuclei under different combined internal fixation methods. From **Figure 13a**, it can be seen that changes in the anterior and posterior approaches have a certain degree of

fluctuation effect on the biomechanics of the C4-C5 disc nucleus. Firstly, when the posterior approach uses the Margel method for nail insertion and the anterior approach replaces parallel nail placement with oblique nail placement (Scheme A–C), the maximum stress on the nucleus increases by about 0.035 MPa, mainly during cervical lateral bending. It can also be observed that in this case, the stress decreases during leftward bending and increases during rightward bending. Secondly, when the posterior approach uses the Anderson method for nail insertion and the anterior approach replaces parallel nail placement with oblique nail placement (Scheme B–D), the maximum stress on the nucleus increases by about 0.024 MPa, mainly during cervical lateral bending. It can also be observed that the change from horizontal nail placement to oblique nail placement leads to an increase in stress during leftward bending and a decrease in stress during rightward bending. Similarly, when the anterior approach uses parallel nail insertion and the posterior approach is replaced by the Margel method (Scheme A–B), there is no significant fluctuation in the maximum stress on the C4-C5 disc nucleus; likewise, when the anterior approach uses oblique nail insertion and the posterior approach changes (Scheme C–D), there is no significant change in the maximum stress on the C4-C5 disc nucleus.

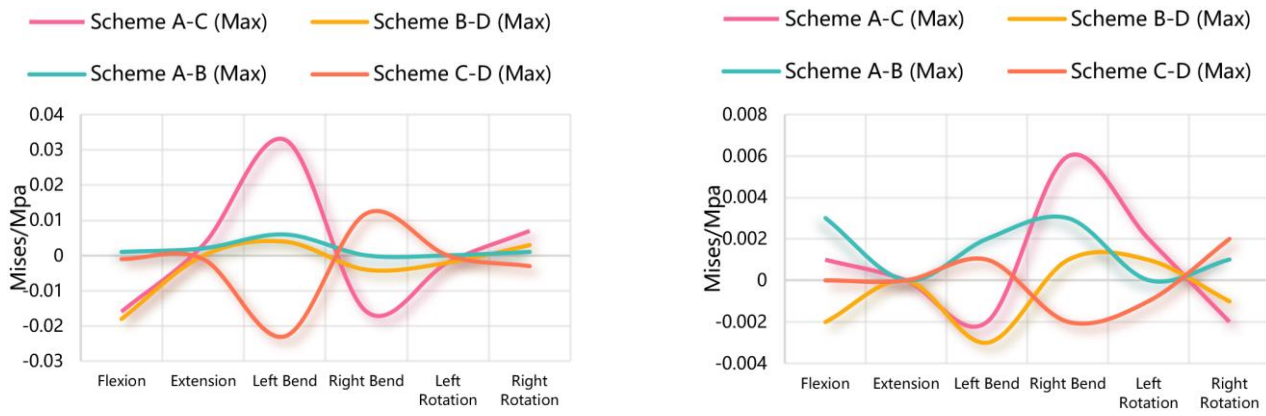

Figure 13. Comparison of maximum stress curves of C5-C6 intervertebral discs. **(a)** stress range curve of C4-C5 intervertebral disc nucleus pulposus; **(b)** stress range curve of the nucleus pulposus of the intervertebral disc.

From **Figure 13b**, it can be seen that the combination of different combined internal fixation methods has a relatively small effect on the biomechanical characteristics of the C6-C7 disc nucleus. When the posterior approach uses the Margel method for nail insertion and the anterior approach replaces parallel nail placement with oblique nail placement (Scheme A–C), the maximum stress on the nucleus increases by about 0.006 MPa, mainly during rightward bending. The variation in other anterior and posterior nail placement methods did not have a significant effect on the biomechanics of the C6-C7 disc nucleus.

Zeng Hongsheng's team analyzed the effectiveness and safety of anterior-posterior combined surgeries for treating cervical spine fractures. Employing anterior-posterior combined surgeries for cervical spine fractures notably enhances surgical efficacy. Among 26 patients, postoperative spinal cord neurologic function improved to a certain extent in 22 cases, with no significant changes observed in 4 cases. During a 16-month follow-up postoperatively, pain scores and cervical disability function

scores significantly decreased compared to preoperative levels in 30 patients, while orthopedic neurologic function scores significantly improved. However, six patients experienced complications, with an occurrence rate of 20.0%. They showed improvement after symptomatic intervention [45]. Baohui Yang and his team have a research on Anterior-Posterior Approach for Treatment of Ankylosing Spondylitis with Obvious Displaced Lower Cervical Spine Fractures and Dislocations. They confirm that the combined approach has demonstrated advantages such as good stabilization, satisfied fracture healing, and easy postoperative cares. However, the difficulty and risk of this approach should be considered. Attention should be paid to the prevention of perioperative complications [46].

It is evident that the impact of postoperative complications on adjacent segments cannot be overlooked when employing the combined approach surgery. The results of this study indicate that, when the anterior approach changes from parallel to inclined placement of screws, there is a noticeable increase in the maximum stress on the C4-C5 nucleus pulposus, particularly during cervical spine lateral bending movements. However, variations in the combined anterior-posterior screw placement do not significantly affect the biomechanics of the C6-C7 nucleus pulposus. These theoretical findings can serve as a reference for the selection of surgical approaches for clinical patients. Additionally, they are beneficial in reducing the likelihood of postoperative complications in patients undergoing anterior-posterior combined procedures.

4.2. Analysis of the interaction between anterior and posterior internal fixation

4.2.1. Analysis of the influence of the anterior nail placement method on posterior internal fixation

To better describe the degree of mutual influence, this section introduces the influence ratio coefficient T. T is the ratio of the difference between the maximum stress values of the two schemes and their arithmetic mean. The specific calculation results are shown in **Figure 14**.

Figure 14a represents the curve of the maximum stress impact of two different posterior screw insertion methods resulting from changes in the anterior screw placement method. **Figure 14b** represents the curve of the maximum stress impact of posterior screw insertion method changes when the anterior screw placement is parallel or tilted. **Figure 14c** represents the curve of the maximum stress impact of titanium rods resulting from changes in the anterior screw placement method for two different posterior screw insertion methods. **Figure 14d** represents the curve of the maximum stress impact of titanium rods resulting from changes in the posterior screw insertion method when the anterior screw placement is parallel or tilted.

In **Figure 14a**, it can be seen that changes in the anterior screw placement method have a relatively small impact on the maximum stress value of the posterior screws, with impact coefficients mostly below 0.05. Among them, the Margel method is slightly more affected by the anterior screw placement changes compared to the Anderson method. The Margel method is most affected during right rotation of the neck, followed by left-side movement. On the other hand, the Anderson method is most affected during neck extension, followed by left-side movement.

Figure 14b represents the degree of influence on the posterior internal fixation system when the posterior screw insertion method changes based on whether the anterior screw placement is parallel or tilted. Firstly, it can be seen from the figure that the two impact coefficient curves have similar values. This indicates that regardless of whether the anterior fixation is parallel or tilted, the stress impact of the posterior internal fixation mainly depends on the posterior screw insertion method. This influence is quite significant, with the maximum impact coefficient appearing during right-side neck movement, at around 0.25. The impact coefficient for extension movement is slightly lower, at about 0.2. The smallest impact occurs during left-side movement, with a coefficient as low as 0.04. The average impact coefficient for both cases is around 0.15.

Figure 14c shows that changes in the anterior screw placement method have a relatively small influence on the maximum stress value of the posteriorly connected titanium rods, with impact coefficients mostly below 0.035. The average impact coefficient for the Anderson method is 0.02, slightly higher than the Margel method. In **Figure 14d**, similar to the case of the posterior screws, the stress impact on the posteriorly connected titanium rods mainly depends on the posterior screw insertion method. The situation with the highest impact occurs during neck flexion movement, with an impact coefficient of about 0.083. The impact coefficient tends towards 0 during axial rotation movement. The average impact coefficient for both cases is around 0.04.

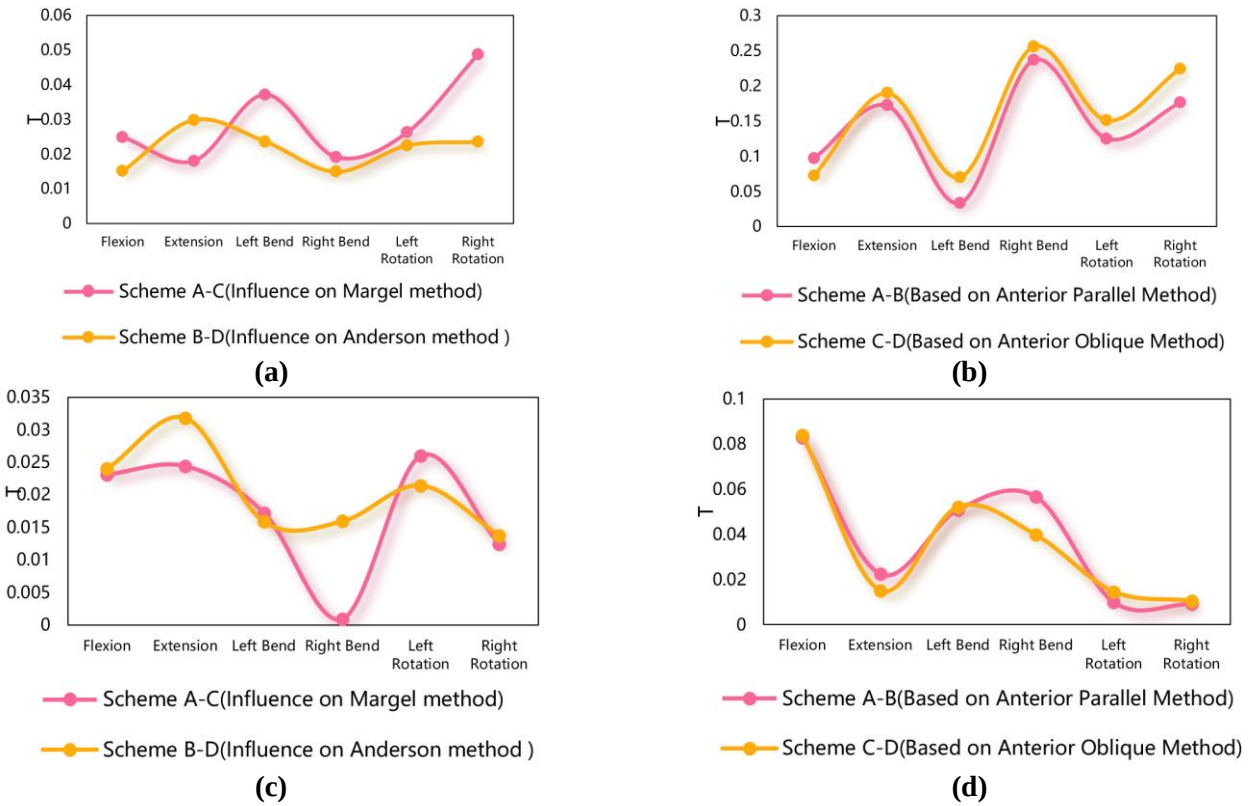

Figure 14. Coefficient of influence of posterior internal fixation system. **(a)** posterior Screw Maximum Stress Impact Curve I; **(b)** posterior Screw Maximum Stress Impact Curve II; **(c)** posterior Titanium Rod Maximum Stress Impact Curve I; **(d)** posterior Titanium Rod Maximum Stress Impact Curve II.

4.2.2. Analysis of the impact of posterior screw insertion methods on anterior internal fixation

Figure 15a represents when the Margel or Anderson method is used to insert the screws in the posterior route, changes in the front pin placement have the maximum stress impact curve on the screw. **Figure 15b** represents when there are changes to the posterior route screw insertion methods, there are different stress impact curves for the two front pin placement methods on the screw. **Figure 15c** represents when the Margel or Anderson method is used to insert the screws in the posterior route, changes in the front pin placement have the maximum stress impact curve on the titanium plate. **Figure 15d** represents when there are changes to the posterior route screw insertion methods, there are different stress impact curves for the two front pin placement methods on the titanium plate.

From **Figure 15a**, it can be observed that when the posterior screw insertion method is Margel, the impact of changes in the anterior screw placement method on the anterior internal fixation screws is significantly smaller compared to when the posterior screw insertion method is Anderson. The latter has a maximum impact coefficient of around 0.82, occurring during left-side neck movement. Its minimum value also exceeds 0.25, occurring during left rotation of the neck. When the posterior screw insertion method is Anderson, the average impact coefficient for the anterior internal fixation system with parallel or tilted screw placement is approximately 0.49. The maximum impact coefficient is only about 0.2, occurring during right-side cervical movement. The minimum impact coefficient tends towards 0. The average impact coefficient is around 0.1.

From **Figure 15b**, with different posterior screw insertion methods, there will be a certain degree of impact on the maximum stress of the anterior internal fixation system for some work conditions with parallel or tilted screw placement. Moreover, the influence trend on the maximum stress of the two anterior screw insertion methods under different cervical movements is basically the same. Among them, when the neck rotates to the left, the maximum stress impact on the anterior internal fixation screws with parallel screw placement is more significant when the posterior screw insertion method is either Margel or Anderson. The impact coefficient is about 0.15. Under the same conditions, the stress impact on the anterior screw with tilted placement is also maximized, with an impact coefficient of about 0.29. The impact coefficient for flexion-extension movement tends towards 0 for both cases. In addition, the average impact coefficients for the parallel and tilted screw placement in the anterior internal fixation screws affected by the posterior screw insertion methods are 0.03 and 0.12, respectively.

As shown in **Figure 15c**, whether the posterior screw insertion method is Margel or Anderson, the stress impact on the anterior plate mainly depends on the anterior screw placement method. The maximum impact occurs during extension and left-side movement of the neck, with a value of about 0.2. The average impact coefficients for both cases are around 0.1. From **Figure 15d**, it can be seen that changes in the posterior screw insertion method have a very small impact on the stress of the anterior plate for both anterior screw placement methods. The maximum value of the impact coefficient is 0.024, appearing respectively in the left rotation movement of the neck for the

parallel placement of the front pins and the forward bending movement for the tilted placement of the pins. The average impact coefficient for these two situations tends towards 0.01 and has almost no effect.

Ram Kumar studied the treatment of cervical degenerative diseases using anterior cervical discectomy and fusion. The results indicated that the stress on Ti screws ranged from 84 MPa to 121 MPa, which is significantly below their yield stress. The study employed an internal fixation method, and the stress results were not compared with relevant approaches for entry route fixation [47]. Duan Y's team compared the postoperative stress levels of three internal fixation techniques. The results indicated that, with the pedicle screw technique and lateral mass screw technique, there was a concentration of high stress at the screw-cap screw-rod interface. The Trans articular Screw (TS) technique caused significant stress differences compared to cervical posterior fixation techniques, mainly manifesting in higher stress levels on the fixation device. The study results elucidate the postoperative scenarios of three different single-entry surgeries. For clinically complex or specific cervical injuries, it is advisable to consider theoretical comparative analyses when contemplating combined surgical approaches [48].

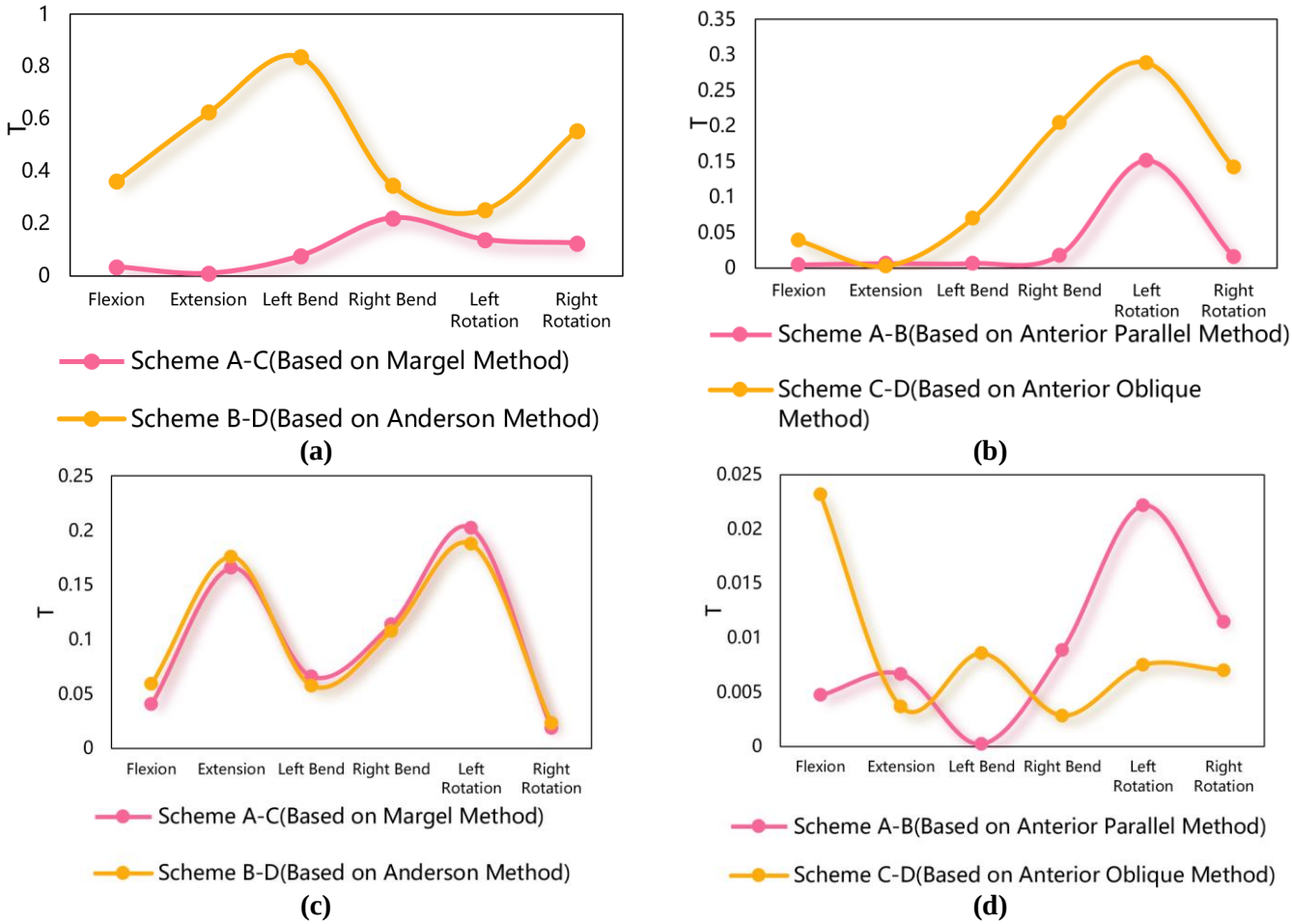

Figure 15. The coefficient of the influence degree of the front internal fixation system. **(a)** anterior Screw Maximum Stress Impact Curve I; **(b)** anterior Screw Maximum Stress Impact Curve II; **(c)** anterior Titanium Rod Maximum Stress Impact Curve I; **(d)** anterior Titanium Rod Maximum Stress Impact Curve II.

Kim GU compared the clinical, radiological, and surgical outcomes of combined approach versus solely posterior approach surgeries. Analyzing 63 patients with cervical myelopathy, the combined approach group exhibited significantly lower posterior neck pain intensity compared to the solely posterior approach group. The rate of screw loosening and implant-related issues in the solely posterior approach group was approximately 40% higher than in the combined approach group. For cervical myelopathy, anterior-posterior cervical fusion yields superior clinical and radiological outcomes compared to posterior fusion alone. However, further in-depth theoretical analysis of the systematic aspects of anterior-posterior fusion surgeries is still needed [49].

The stress levels of various combined approach surgical internal fixation devices have been detailed in the results section of this article. Through a thorough comparative discussion, this study has further elucidated the mutual impact of anterior and posterior approaches on the stress of the instrumentation. Changes in the front pin insertion method have relatively little impact on the maximum stress values of the posterior route screws and connecting titanium rods. The main factor depends on the posterior route screw insertion method, and the maximum impact coefficient reaches 0.25, appearing in the right rotation movement of the neck. When the Margel method is used to insert screws in the posterior route, changes in the front pin placement have a significantly smaller impact on the stress of the screw in the front internal fixation system than when the Anderson method is used in the posterior route. The latter has a maximum impact coefficient of 0.82, appearing in the left rotation movement of the neck. As the posterior route insertion method changes, it will have a certain degree of impact on the maximum stress of the front internal fixation system in the partially employed work conditions of the parallel or tilted pin placement. The latter's maximum affected coefficient is 0.29, occurring in the left rotation movement. The stress impact on the front connecting titanium plate mainly depends on the front pin insertion method. Its maximum affected value is 0.2. Changes in the posterior route screw insertion method have little effect on it.

4.2.3. Analyses of the critical torque of the posterior route internal fixation locking nut

Kim GU compared the clinical, radiological, and surgical outcomes of combined approaches with solely posterior approaches. An analysis of 63 patients with cervical myelopathy revealed significantly lower levels of posterior neck pain intensity in the combined approach group compared to the solely posterior approach group. In the solely posterior approach group, the incidence of screw loosening and implant-related issues reached 60%. This figure was 21% in the combined anterior-posterior approach group [49].The study by Coe JD demonstrated that in patients undergoing posterior cervical interbody fusion surgery, less than 1% experienced instrumentation complications such as screw or rod protrusion, screw or plate breakage, and screw loosening [50].The clinical study by Tomoaki Shimizu on posterior cervical fusion surgery revealed that out of 94 surgical cases involving the clinical utility of paravertebral foramen screws, three cases experienced screw loosening [51].

From this perspective, further in-depth research is needed on theoretical analyses related to the stability of internal fixation systems. This study aims to calibrate the

minimum torque of posterior locking nuts by combining biomechanical interactions with the interactions between anterior and posterior instrumentation. The equivalent stress cloud maps related to the four combined internal fixation methods were obtained by finite element model calculations for 6 cervical movements. The mean value of the dangerous cross-sectional stress of the locking nut used for limiting and fastening the posterior route titanium rod is shown in **Table 5**. The stress value of the dangerous cross-section of the nut under different working conditions is basically distributed in the range of 19 Mpa–25 Mpa. By converting the bolt cross-sectional pressure into a load and considering the safety factor of the actual working conditions, the minimum preload required for the nut under the action of each cervical movement was calculated. Its value is basically distributed between 1100 N–1500 N.

Table 5. Dangerous section stress and minimum preload of set screw.

	Scheme	**Flexion**	**Extension**	**Left Bend**	**Right Bend**	**Left Rotation**	**Right Rotation**
Stress value of dangerous section/Mpa	A	21.2	25.3	23.2	20.8	25.5	18.6
	B	23.1	26.6	24.6	19.9	26.1	19.0
	C	21.9	25.9	23.7	20.9	26.2	19.1
	D	23.8	27.5	25.0	20.3	26.8	19.4
Minimum preload/N	A	1307.2	1560.3	1431.0	1283.2	1570.8	1144.1
	B	1422.4	1640.4	1512.3	1227.8	1605.9	1172.4
	C	1346.6	1592.3	1458.7	1288.8	1614.5	1177.9
	D	1464.9	1691.5	1541.8	1249.4	1648.4	1192.1

The calculation formula for bolt preload force and tightening torque is shown.

$$T = \frac{1}{2} F_0 \left[d\tan(\phi + \psi_v) + \frac{2}{3} f_c \frac{D^3 - d^3}{D^2 - d^2} \right]$$

F_0 is the bolt preload force, d is the thread diameter, D is the outer diameter of the annular support surface, φ is the thread angle, ψ_v is the equivalent friction angle, and f_c is the friction coefficient between the nut and the support surface. The results of the tightening torque calculation for the nut are shown in **Figure 16**, which shows the stress cross-section of the traditional titanium plate split line.

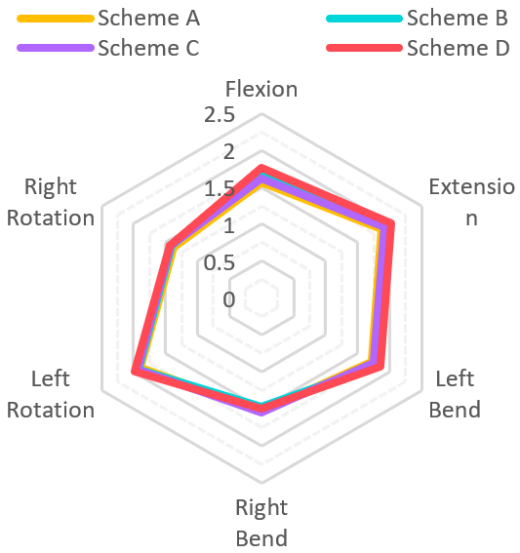

Figure 16. Stress cross section of traditional titanium plate.

It can be seen from the **Figure 16** that the minimum critical torque distribution trends of the locking nuts for the posterior route for the four combined surgical methods are basically the same under the six cervical movement conditions. Among them, the required torque reaches the maximum in the left rotation and extension movements, with a value of about 2.1 nm. The minimum torque is 1.4 nm for the right rotation movement. In summary, for the internal fixation situation of the four combined anterior-posterior route surgeries studied in this article, it is recommended to use a torque of at least 2.1 nm to tighten the locking nut of the posterior route titanium rod.

5. Conclusion

This article established a finite element model after C3-C7 anterior and posterior combined surgery and completed relevant validation and calculation result analysis. It drew conclusions on the biomechanics of adjacent segment intervertebral disc nuclei and the mutual influence of stresses on anterior and posterior internal fixation devices.

In terms of biomechanics, when the angle of the anterior fixation nail insertion is tilted, it significantly increases the maximum stress on the C4-C5 disc nucleus. However, it does not have a significant impact on the biomechanics of the C6-C7 disc nucleus. In clinical practice, it is theoretically preferable to maintain horizontal nail insertion. At the same time, it is necessary to pay attention to the degeneration of adjacent segment intervertebral disc nuclei and other symptoms in patients after surgery.

In terms of internal fixation devices, changes in the anterior nail insertion method have a minimal effect on the stress on the posterior screws and connecting titanium rods. Compared to the Margel method, the Anderson method has a greater impact on the stress on the anterior fixation screws. In clinical practice, while selecting a combined surgical plan based on the patient's lesions, the interaction between the anterior and posterior internal fixation systems should not be overlooked. This helps improve the overall stability and service life of the internal fixation system. Additionally, in the four combined anterior and posterior surgery scenarios studied in

this article, applying a torque of at least 2.1 nm to lock the nuts of the posterior titanium rods can effectively ensure the stability of the internal fixation system.

Author contributions: Conceptualization, DL and KW; methodology, CD; software, DL; validation, DL, KW and CD; formal analysis, BZ; investigation, LG; resources, HY; data curation, DL; writing—original draft preparation, KW; writing—review and editing, HY; visualization, CD; supervision, BZ; project administration, DL; funding acquisition, DL. All authors have read and agreed to the published version of the manuscript.

Availability of data and materials: The data and materials of this study are available from the corresponding author.

Funding: This research was funded the Natural Science Foundation of Hunan Province under Project, Grant Number 2022JJ60072.

Ethical approval: The study was conducted in accordance with the Declaration of Helsinki, and approved by the Institutional Review Board of HUNAN RAILWAY PROFESSIONAL TECHNOLOGY COLLEGE (protocol code HNRPC.05.43 and 2023.02.04). Informed consent was obtained from all subjects involved in the study.

Conflict of interest: The authors declare no conflict of interest.

References

1. Iencean SM. Double noncontiguous cervical spinal injuries. Acta neurochirurgica. 2002; 144(7): 695-701. doi: 10.1007/s00701-002-0940-7
2. Seçer M, Alagöz F, Uçkun O, et al. Multilevel Noncontiguous Spinal Fractures: Surgical Approach towards Clinical Characteristics. Asian Spine Journal. 2015; 9(6): 889. doi: 10.4184/asj.2015.9.6.889
3. Passias PG, Poorman GW, Segreto FA, et al. Traumatic Fractures of the Cervical Spine: Analysis of Changes in Incidence, Cause, Concurrent Injuries, and Complications Among 488,262 Patients from 2005 to 2013. World Neurosurgery. 2018; 110: e427-e437. doi: 10.1016/j.wneu.2017.11.011
4. Zileli M, Osorio-Fonseca E, Konovalov N, et al. Early Management of Cervical Spine Trauma: WFNS Spine Committee Recommendations. Neurospine. 2020; 17(4): 710-722. doi: 10.14245/ns.2040282.141
5. Ngo LM, Aizawa T, Hoshikawa T, et al. Fracture and contralateral dislocation of the twin facet joints of the lower cervical spine. European Spine Journal. 2011; 21(2): 282-288. doi: 10.1007/s00586-011-1956-6
6. Yang H, Wang H, Zhang B, et al. Cervical spine fracture-dislocation in patients with ankylosing spondylitis and severe thoracic kyphosis: Application of halo vest before and during surgical management. Clinical Neurology and Neurosurgery. 2021; 207: 106744. doi: 10.1016/j.clineuro.2021.106744
7. Mu X, Li Z, Ou Y, et al. Early and short-segment anterior spinal fusion for cervical spinal cord injury without fracture and dislocation can achieve more significant neurological recovery: a retrospective study based on the current medical system in southern China. Journal of Orthopaedic Surgery and Research. 2019; 14(1). doi: 10.1186/s13018-019-1487-0
8. Liao JC, Fan KF. Posterior short-segment fixation in thoracolumbar unstable burst fractures – Transpedicular grafting or six-screw construct? Clinical Neurology and Neurosurgery. 2017; 153: 56-63. doi: 10.1016/j.clineuro.2016.12.011
9. Miao DC, Qi C, Wang F, et al. Management of Severe Lower Cervical Facet Dislocation without Vertebral Body Fracture Using Skull Traction and an Anterior Approach. Medical Science Monitor. 2018; 24: 1295-1302. doi: 10.12659/msm.908515
10. Wang J, Li J, Cai L. Effects of Treatment of Cervical Spinal Cord Injury without Fracture and Dislocation in A Medium-to Long-Term Follow-Up Study. World Neurosurgery. 2018; 113: e515-e520. doi: 10.1016/j.wneu.2018.02.071
11. Lee S, Kim C, Ha JK, et al. Comparison of Early Surgical Treatment with Conservative Treatment of Incomplete Cervical Spinal Cord Injury Without Major Fracture or Dislocation in Patients with Pre-existing Cervical Spinal Stenosis. Clinical Spine Surgery: A Spine Publication. 2020; 34(3): E141-E146. doi: 10.1097/bsd.0000000000001065

12. Aebi M. Surgical treatment of upper, middle and lower cervical injuries and non-unions by anterior procedures. European Spine Journal. 2009; 19(S1): 33-39. doi: 10.1007/s00586-009-1120-8
13. Liu K, Zhang Z. Comparison of a novel anterior-only approach and the conventional posterior–anterior approach for cervical facet dislocation: a retrospective study. European Spine Journal. 2019; 28(10): 2380-2389. doi: 10.1007/s00586-019-06073-3
14. Yu ZS, Yue JJ, Wei F, et al. Treatment of cervical dislocation with locked facets. Chinese Medical Journal. 2007; 120(3): 216-218. doi: 10.1097/00029330-200702010-00008
15. Garvey TA, Eismont FJ, Roberti LJ. Anterior Decompression, Structural Bone Grafting, and Caspar Plate Stabilization for Unstable Cervical Spine Fractures and/or Dislocations. Spine. 1992; 17(Supplement): S431-S435. doi: 10.1097/00007632-199210001-00015
16. Liu K, Zhang Z. A Novel Anterior-Only Surgical Approach for Reduction and Fixation of Cervical Facet Dislocation. World Neurosurgery. 2019; 128: e362-e369. doi: 10.1016/j.wneu.2019.04.153
17. Chen M, Wang Z, Fan Y, et al. Nursing Care of a Patient with Cervical Spinal Cord Injury Without Fracture and Dislocation: A Case Report. American Journal of Nursing Science. 2020; 9(5): 352. doi: 10.11648/j.ajns.20200905.16
18. Schleicher P, Kobbe P, Kandziora F, et al. Treatment of Injuries to the Subaxial Cervical Spine: Recommendations of the Spine Section of the German Society for Orthopaedics and Trauma (DGOU). Global Spine Journal. 2018; 8(2_suppl): 25S-33S. doi: 10.1177/2192568217745062
19. Alam N, Haque MR, Kamaluddin M, et al. Cervical spinal injury: experience with 82 cases. International Congress Series. 2002; 1247(1): 591-596.
20. Brodke DS, Zdeblick TA. Modified Smith-Robinson Procedure for Anterior Cervical Discectomy and Fusion. Spine. 1992; 17(Supplement): S427-S430. doi: 10.1097/00007632-199210001-00014
21. Rao RD, Wang M, McGrady LM, et al. Does Anterior Plating of the Cervical Spine Predispose to Adjacent Segment Changes? Spine. 2005; 30(24): 2788-2792. doi: 10.1097/01.brs.0000190453.46472.08
22. Theodotou CB, Ghobrial GM, Middleton AL, et al. Anterior Reduction and Fusion of Cervical Facet Dislocations. Neurosurgery. 2018; 84(2): 388-395. doi: 10.1093/neuros/nyy032
23. Johnson MG, Fisher CG, Boyd M, et al. The Radiographic Failure of Single Segment Anterior Cervical Plate Fixation in Traumatic Cervical Flexion Distraction Injuries. Spine. 2004; 29(24): 2815-2820. doi: 10.1097/01.brs.0000151088.80797.bd
24. Song KJ, Lee KB. Anterior versus combined anterior and posterior fixation/fusion in the treatment of distraction-flexion injury in the lower cervical spine. Journal of Clinical Neuroscience. 2008; 15(1): 36-42. doi: 10.1016/j.jocn.2007.05.010
25. Lee JY, Nassr A, Eck JC, et al. Controversies in the treatment of cervical spine dislocations. The Spine Journal. 2009; 9(5): 418-423. doi: 10.1016/j.spinee.2009.01.005
26. Cybulski GR, Douglas RA, Meyer PR, et al. Complications in Three-Column Cervical Spine Injuries Requiring Anterior–Posterior Stabilization. Spine. 1992; 17(3): 253-256. doi: 10.1097/00007632-199203000-00001
27. Henriques T, Olerud C, Bergman A, et al. Distractive Flexion Injuries of the Subaxial Cervical Spine Treated With Anterior Plate Alone. Journal of Spinal Disorders & Techniques. 2004; 17(1): 1-7. doi: 10.1097/00024720-200402000-00002
28. Ren C, Qin R, Wang P, et al. Comparison of anterior and posterior approaches for treatment of traumatic cervical dislocation combined with spinal cord injury: Minimum 10-year follow-up. Scientific Reports. 2020; 10(1). doi: 10.1038/s41598-020-67265-2
29. Zhou Q, Zhang J, Liu H, et al. Comparison of Anterior and Posterior Approaches for Acute Traumatic Central Spinal Cord Syndrome with Multilevel Cervical Canal Stenosis without Cervical Fracture or Dislocation. Mouzopoulos G, ed. International Journal of Clinical Practice. 2022; 2022: 1-11. doi: 10.1155/2022/5132134
30. He A, Xie D, Cai X, et al. One-stage surgical treatment of cervical spine fracture-dislocation in patients with ankylosing spondylitis via the combined anterior–posterior approach. Medicine. 2017; 96(27): e7432. doi: 10.1097/md.0000000000007432
31. Molinari L, Falcinelli C, Gizzi A, et al. Biomechanical modeling of metal screw loadings on the human vertebra. Acta Mechanica Sinica. 2021; 37(2): 307-320. doi: 10.1007/s10409-021-01063-5
32. Karim SMdR, Rahman AKMS, Sobhan SA, et al. Outcome of Long Segment Transpedicular Screw Fixation in Unstable Thoracolumbar Spine Injury with Incomplete Neurological Deficit. Journal of Biosciences and Medicines. 2020; 08(03): 166-187. doi: 10.4236/jbm.2020.83015
33. Wang X, Feng M, Hu Y. Establishment and Finite Element Analysis of a Three-dimensional Dynamic Model of Upper Cervical Spine Instability. Orthopaedic Surgery. 2019; 11(3): 500-509. doi: 10.1111/os.12474

34. Yoganandan N, Kumaresan S, Voo L, et al. Finite Element Model of the Human Lower Cervical Spine: Parametric Analysis of the C4-C6 Unit. Journal of Biomechanical Engineering. 1997; 119(1): 87-92. doi: 10.1115/1.2796070
35. Do Koh Y, Lim TH, Won You J, et al. A Biomechanical Comparison of Modern Anterior and Posterior Plate Fixation of the Cervical Spine. Spine. 2001; 26(1): 15-21. doi: 10.1097/00007632-200101010-00005
36. Ebraheim NA, Klausner T, Xu R, et al. Safe Lateral-Mass Screw Lengths in the Roy-Camille and Magerl Techniques. Spine. 1998; 23(16): 1739-1742. doi: 10.1097/00007632-199808150-00006
37. Magerl F. Stable posterior fusion of the atlas and axis by trans articular screw fixation. Cervical Spine. 1987; 1: 322-327.
38. Ren G, Wang G, Xiao B, et al. The use of cervical lateral mass plate and screw for the treatment of fracture and dislocation of the lower cervical spine. Journal of Practical Orthopaedics. 2007; 13(5): 259-261.
39. Anderson pa, Henley MB, Grady MS, et al. Posterior Cervical Arthrodesis with AO Reconstruction Plates and Bone Graft. Spine. 1991; 16: S72-S79.
40. Zhang QH, Teo EC, Ng HW. Development and Validation of a C0–C7 FE Complex for Biomechanical Study. Journal of Biomechanical Engineering. 2005; 127(5): 729-735. doi: 10.1115/1.1992527
41. Yoganandan N, Kumaresan S, Pintar FA. Biomechanics of the cervical spine Part 2. Cervical spine soft tissue responses and biomechanical modeling. Clinical biomechanics (Bristol, Avon). 2001; 16(1): 1-27.
42. Hong-Wan N, Ee-Chon T, Qing-Hang Z. Biomechanical Effects of C2–C7 Intersegmental Stability due to Laminectomy with Unilateral and Bilateral Facetectomy. Spine. 2004; 29(16): 1737-1745. doi: 10.1097/01.brs.0000134574.36487.eb
43. Moroney SP, Schultz AB, Miller JA, Andersson GB. Load-displacement properties of lower cervical spine motion segments. Journal of biomechanics, 21(9), 769-779.
44. Panjabi M, Brand R, White A. Mechanical properties of the human thoracic spine as shown by three-dimensional load-displacement curves. The Journal of Bone & Joint Surgery. 1976; 58(5): 642-652. doi: 10.2106/00004623-197658050-00011
45. Zeng HS, Jin J, Chen ZJ, Chen XY. Analysis of the effect and safety of anterior and posterior combined surgery for the treatment of cervical spine fractures in ankylosing spondylitis. Heilongjiang Medicine. 2023; (03): 534-538.
46. Yang B, Lu T, Li H. Single-Session Combined Anterior-Posterior Approach for Treatment of Ankylosing Spondylitis with Obvious Displaced Lower Cervical Spine Fractures and Dislocations. BioMed Research International. 2017; 2017: 1-7. doi: 10.1155/2017/9205834
47. Kumar R, Kumar A. Biomechanical analysis of a single-level customized cage screw fixation for anterior cervical discectomy and fusion in the cervical spine: an in-silico study. Biomedical Physics & Engineering Express. 2023; 9(4): 045018. doi: 10.1088/2057-1976/acd784
48. Duan Y, Zhang H, Min SX, et al. Posterior cervical fixation following laminectomy: a stress analysis of three techniques. European Spine Journal. 2011; 20(9): 1552-1559. doi: 10.1007/s00586-011-1711-z
49. Kim GU, Ahn MW, Lee GW. Combined Anterior-Posterior Fusion Versus Posterior Alone Fusion for Cervical Myelopathy in Athetoid-Cerebral Palsy. Global Spine Journal. 2021; 12(8): 1715-1722. doi: 10.1177/2192568220987535
50. Coe JD, Vaccaro AR, Dailey AT, et al. Lateral Mass Screw Fixation in the Cervical Spine. The Journal of Bone & Joint Surgery. 2013; 95(23): 2136-2143. doi: 10.2106/jbjs.l.01522
51. Shimizu T, Koda M, Abe T, et al. Paravertebral foramen screw fixation for posterior cervical spine surgery: clinical case series. Journal of Neurosurgery: Spine. 2022; 36(3): 479-486. doi: 10.3171/2021.6.spine21411